Circuits Syst Signal Process
DOI 10.1007/s00034-008-9045-8

A Novel Diversity-Controlled Genetic Algorithm for Rapid Optimization of Bandpass FRM FIR Digital Filters Over CSD Multiplier Coefficient Space

Sai Mohan Kilambi · Behrouz Nowrouzian · Yifan Wu

Received: 27 March 2007 / Revised: 10 February 2008
© Birkhäuser Boston 2008

Abstract The conventional frequency response masking (FRM) approach is one of the most well-known techniques for the design of sharp transition band finite impulse response (FIR) digital filters. The resulting FRM digital filters permit efficient hardware implementations due to an inherently large number of *zero-valued* multiplier coefficients. The hardware complexity of these digital filters can further be reduced by representing the remaining (non-zero) multiplier coefficient values by using their canonical signed-digit (CSD) representations. This paper presents a novel diversity-controlled (DC) genetic algorithm (GA) for the discrete optimization of bandpass FRM FIR digital filters over the CSD multiplier coefficient space. The resulting bandpass FIR digital filters are permitted to have equal or unequal lower and upper transition bandwidths. The proposed DCGA is based on an indexed look-up table of permissible CSD multiplier coefficients such that their indices form a closed set under the genetic operations of crossover and mutation. The salient advantage of DCGA over the conventional GA lies in the external control over population diversity and parent selection, giving rise to a rapid convergence to an optimal solution. The external control is achieved through the judicious choice of a pair of DCGA optimization parameters. An empirical investigation is undertaken for choosing appropriate values for these control parameters. The convergence speed advantages of the DCGA are demonstrated through its application to the design and optimization of a pair of bandpass FRM FIR digital filters with equal or arbitrary lower and upper transition

S.M. Kilambi
Nortel Networks Ltd, Ottawa, ON, Canada
e-mail: skilambi@nortel.com

B. Nowrouzian (✉) · Y. Wu
Department of Electrical and Computer Engineering, University of Alberta, Edmonton, AB, Canada
e-mail: nowr@ece.ualberta.ca

Y. Wu
e-mail: yifan2@ualberta.ca

bandwidths. In both cases, an increase of about an order of magnitude in the speed of convergence is achieved as compared to the conventional GAs.

Keywords FRM approach · FIR digital filters · DCGAs · CSD number system

1 Introduction

A vast body of literature is available for the design and optimization of linear phase finite impulse response (FIR) digital filters. These digital filters exhibit guaranteed non-linear/linear stability features and low coefficient sensitivities, in addition to possessing constant group delays [15]. Linear phase FIR digital filters with sharp transition bands find many important practical applications, e.g. in digital audio systems [7]. However, the order of such filters is usually inversely proportional to the width of their transition bands, implying that their orders become prohibitively large for narrow transition bandwidths. Since the number of addition and multiplication operations carried out by the digital filter in each sampling interval is directly proportional to the filter order, FIR digital filters with large orders entail high computational complexities. To this end, plenty of research has been directed towards developing new design techniques which reduce the computational complexity of linear phase FIR digital filters having sharp transition bands (e.g. [16]).

The frequency response masking (FRM) approach is one of the most efficient techniques for the design of sharp transition band FIR digital filters. Given a set of design specifications, the order of an FRM FIR digital filter is only slightly longer than that of the corresponding conventional direct-form FIR digital filter. This is made possible by realizing a sharp transition band FRM FIR digital filter in terms of a combination of a pair of interpolated bandedge shaping and a corresponding pair of gradual-transition band masking FIR digital sub-filters. This causes a substantial reduction in the computational complexity of the overall FRM FIR digital filter, mainly due to a relatively large number of zero-valued multiplier coefficients in the constituent interpolated FIR digital sub-filters [8].

The non-zero valued multiplier coefficients in FRM FIR digital filters can be determined in *infinite precision* by separate optimization of the masking and bandedge shaping digital sub-filters, e.g. by using the existing gradient-based optimization techniques such as the Parks–McClellan approach. Other gradient-based optimization techniques for FRM digital filters include the weighted least-squares approach [23] and the semi-definite [12] and second-order cone programming [13] approaches. Recently, a more attractive technique based on non-linear programming was developed [17] (see also [22]) for the joint optimization of the constituent digital sub-filters, leading to a substantial reduction in the number of addition and multiplication operations in the realization of the overall FRM digital filter. A further reduction was also possible by constructing the corresponding masking digital sub-filters in terms of a common part.

In an actual hardware/software implementation of the FRM FIR digital filter, the constituent non-zero valued multiplier coefficients are quantized to their finite-precision counterparts, e.g. by using their signed-power-of-two (SPT) representations [11]. The SPT multiplier coefficient value representation leads to a multiplier-free digital filter, as made possible by replacing the required multiplication operations

by a finite number of shift and add operations [24]. In [6], a simulated annealing approach was developed for the discrete optimization of FRM digital filters over the SPT multiplier coefficient space.

The SPT representation of a given number is non-unique, causing redundancy in the multiplier coefficient representation. This redundancy can potentially increase the corresponding computational complexity due to repetitive recourse to the "compare" logic operation. In order to circumvent this problem, one may resort to special cases of the SPT number system, e.g. the canonical signed-digit (CSD) or the canonical double-base number systems [2, 3]. These number systems are capable of representing multiplier coefficient values uniquely by restricting the resulting number of non-zero digits.

After the quantization of the infinite-precision multiplier coefficient values, the frequency response of the FRM FIR digital filter may no longer satisfy the initial design specifications. As a result, optimization techniques have to be employed once again to obtain a finite-precision digital filter that satisfies the given design specifications.

In [10], it was demonstrated that, by using integer programming over the SPT multiplier coefficient space, the frequency response of FIR digital filters can be optimized to meet very stringent design specifications. In the case of FRM FIR digital filters, however, this optimization technique proves to be time consuming and results in sub-optimal solutions. This generally stems from a separate optimization of the constituent digital sub-filters.

Genetic algorithms (GAs) have emerged as an efficient alternative for the optimization of both finite-precision FIR and infinite impulse response digital filters [3, 20]. These algorithms are based on an evolution of a population pool consisting of candidate solutions from one generation to the next in the process of arriving at the desired optimal solution. GAs are capable of automatically finding near-optimum solutions to discrete optimization problems while keeping the computational cost low [20]. In [25], a GA was applied to the design of an SPT quadrature mirror lattice filter bank.

The conventional GAs do not search the solution space robustly, mainly due to a lack of mechanisms through which entrapment at local optima can be successfully avoided. In [1], a simulated annealing approach was employed to improve the convergence speed.

In [18, 19], Shimodaira developed a diversity-controlled (DC) GA that circumvents the problem of convergence speed by allowing external control over the diversity of the population pool. This external control prevents premature convergence to a local optimal solution, increasing the speed of convergence of the DCGA towards a global optimum solution.

In this paper, the DCGA approach is exploited for the design and optimization of bandpass FRM FIR digital filters over the fixed radix point CSD multiplier coefficient space, where the multiplier coefficients are permitted to have a prespecified wordlength W, and a prespecified *maximum* number of non-zero digits w. Moreover, an empirical investigation is undertaken for the judicious choice of the DCGA control parameters for rapid optimization of FRM FIR digital filters.

The rest of this paper is organized as follows: Sect. 2 is concerned with the design of bandpass FRM FIR digital filters with equal or arbitrary upper and lower transition

bandwidths. Section 3 presents a review of the DCGA together with a discussion of the effect of the corresponding control parameters on the speed of convergence. Section 4 presents the details of the proposed DCGA for the optimization of finite-precision FRM FIR digital filters. Section 5 illustrates the proposed GA optimization through its application to the design of a pair of bandpass FRM FIR digital filters with equal and unequal lower and upper transition bands over the CSD multiplier coefficient space. Empirical results are also given for selecting the DCGA control parameters. Section 6 summarizes the main conclusions of the paper.

2 Design of Bandpass FRM FIR Digital Filters

The conventional FRM approach [8] concerns the design of lowpass FIR digital filters in terms of a pair of interpolated bandedge shaping and a corresponding pair of lowpass masking digital sub-filters. This approach can easily be extended to a *direct* design of bandpass (bandstop, respectively) FIR digital filters by employing bandpass (bandstop, respectively) masking digital sub-filters instead [14]. However, the resulting FRM FIR digital filters will exhibit identical lower and upper transition bandwidths.

In order to permit different lower and upper transition bandwidths, one can realize a bandpass (bandstop, respectively) FIR digital filter *indirectly*, i.e. in terms of a cascade (parallel, respectively) combination of a pair of lowpass and highpass FRM FIR digital filters. In [21], the indirect approach was applied to the design of bandstop FIR digital filters employing different interpolation factors for the realization of the constituent lowpass and highpass FIR digital filters. In this paper, a similar approach is developed for the design of the corresponding bandpass FIR digital filters having unequal or equal lower and upper transition bandwidths.

To this end, let the desired bandpass FIR digital filter $H_{\mathrm{BP}}(z) = Y_{\mathrm{BP}}(z)/X_{\mathrm{BP}}(z)$ have a lower transition bandwidth of Δ_{l} and an upper transition bandwidth of Δ_{u}, where $X_{\mathrm{BP}}(z)$ and $Y_{\mathrm{BP}}(z)$ represent, respectively, the input and output signals associated with the bandpass FIR digital filter $H_{\mathrm{BP}}(z)$. Let us decompose $H_{\mathrm{BP}}(z)$ in accordance with

$$H_{\mathrm{BP}}(z) = H_{\mathrm{LP}}(z)H_{\mathrm{HP}}(z), \tag{1}$$

where $H_{\mathrm{LP}}(z) = Y_{\mathrm{LP}}(z)/X_{\mathrm{LP}}(z)$ represents a lowpass and $H_{\mathrm{HP}}(z) = Y_{\mathrm{HP}}(z)/X_{\mathrm{HP}}(z)$ represents a highpass FRM FIR digital filter. In this way, $H_{\mathrm{LP}}(z)$ is of the form [21]

$$H_{\mathrm{LP}}(z) = z^{\frac{-M_{\mathrm{LP}}(N_{\mathrm{LP}}-1)}{2}} H_{\mathrm{mbl}}(z) + H_{\mathrm{dl}}(z)H_{\mathrm{al}}(z^{M_{\mathrm{LP}}}) \tag{2}$$

where

$$H_{\mathrm{dl}}(z) = H_{\mathrm{mal}}(z) - H_{\mathrm{mbl}}(z), \tag{3}$$

and where N_{LP} represents the order of $H_{\mathrm{al}}(z)$. In (2), $H_{\mathrm{al}}(z^{M_{\mathrm{LP}}})$ represents the M_{LP}-interpolated version of the bandedge shaping digital sub-filter $H_{\mathrm{al}}(z)$, and $H_{\mathrm{mal}}(z)$, $H_{\mathrm{mbl}}(z)$ represent the corresponding lowpass masking digital sub-filters.

The highpass FRM FIR digital filter $H_{\mathrm{HP}}(z)$ in (1) can be represented in much the same way as [21]

$$H_{\mathrm{HP}}(z) = z^{\frac{-M_{\mathrm{HP}}(N_{\mathrm{HP}}-1)}{2}} H_{\mathrm{mbh}}(z) + H_{\mathrm{ah}}(z^{M_{\mathrm{HP}}}) H_{\mathrm{dh}}(z) \tag{4}$$

where

$$H_{\mathrm{dh}}(z) = H_{\mathrm{mah}}(z) - H_{\mathrm{mbh}}(z), \tag{5}$$

and where N_{HP} represents the order of $H_{\mathrm{ah}}(z)$. In (4), $H_{\mathrm{ah}}(z^{M_{\mathrm{HP}}})$ represents the M_{HP}-interpolated version of the bandedge shaping digital sub-filter $H_{\mathrm{ah}}(z)$, and $H_{\mathrm{mah}}(z)$ and $H_{\mathrm{mbh}}(z)$ represent the corresponding highpass masking digital sub-filters.

A first approximation to the optimum value of $M_{\mathrm{LP(HP)}}$ is given by [5, 9]

$$M_{\mathrm{LP(or\ HP)}} = \frac{1}{\sqrt{\alpha \Delta_{\mathrm{l(or\ u)}}}}, \tag{6}$$

where $\alpha = 4$ in the case of a separate optimization of the constituent bandedge shaping and masking digital sub-filters. However, in the case of a joint optimization of the constituent digital sub-filters, an empirical investigation led to $\alpha = 2.25$ in [22], while an analytical investigation in [17] led to $\alpha = 2.4$. In this paper, a better approximation for the interpolation factor M is obtained by tabulating the overall bandpass FRM FIR digital filter order as a function of M_{LP} and M_{HP} in the vicinity of the first approximations for M_{LP} and M_{HP} with $\alpha = 2.4$, and by selecting the M_{LP} and M_{HP} values which lead to a minimum overall FRM digital filter order.

The lower (upper) transition bandwidth $\Delta_{\mathrm{l(u)}}$ is governed by the constituent transition bandwidth of the highpass (lowpass) FRM FIR digital filter.

The realizations for $H_{\mathrm{LP}}(z)$, $H_{\mathrm{HP}}(z)$ and the desired overall $H_{\mathrm{BP}}(z)$ are shown in Figs. 1, 2 and 3.

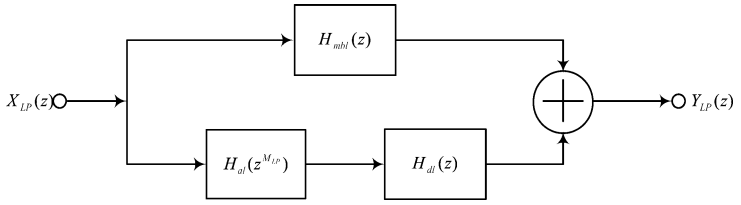

Fig. 1 Realization of lowpass FRM FIR digital filters [21]

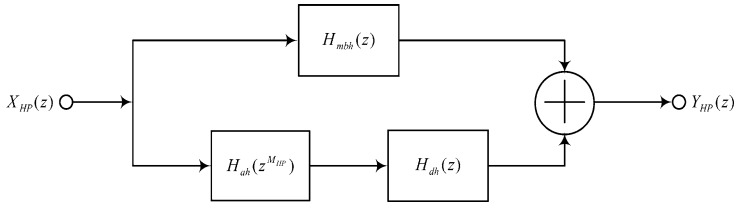

Fig. 2 Realization of highpass FRM FIR digital filters [21]

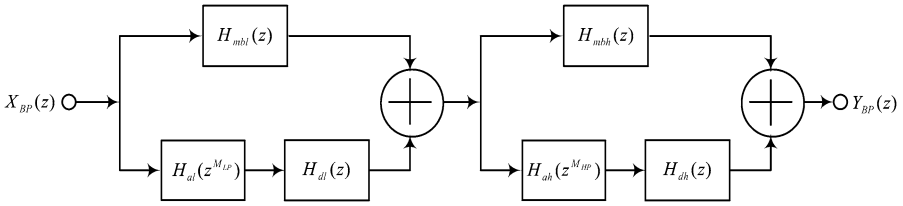

Fig. 3 Synthesis structure for bandpass FRM FIR digital filters

3 Diversity-Controlled GAs

GAs are optimization techniques which are based on the process of natural selection and biological evolution [4, 25]. They begin with a seed chromosome which is usually represented as a bit-string. Then, an initial population pool of additional candidate chromosomes is obtained by randomly complementing bits in the seed chromosome. Based on the initial population pool, the GA proceeds from one generation to the next to arrive at a chromosome representing an optimal solution to the optimization problem.

In order to obtain the next-generation population pool, a mating pool is formed by randomly selecting chromosomes from the current population pool by evaluating their fitness function. Then, pairs of parent chromosomes in the mating pool undergo the process of reproduction by employing the genetic operations of crossover and mutation. The resulting offspring chromosomes become members of the next-generation population pool. In the process of forming the mating pool, *non-elite* chromosomes (i.e. chromosomes with low fitness values) are also added to the population pool in order to increase the population diversity. The genetic operations of crossover and mutation are performed repeatedly from one generation to the next until a prespecified termination condition is reached.

Despite the fact that GAs are excellent choices for discrete optimization problems, they do not search the solution space robustly, mainly due to a lack of mechanisms through which entrapment at *local optima* could be successfully avoided. This leads to *premature convergence,* which is usually the result of a quick decrease in population diversity.

To circumvent this problem, Shimodaira [19] developed the DCGA, where the search is made effective by keeping track of current chromosomes which have low fitness values but which have the potential of evolving to individuals with high fitness values in future generations. In addition, the diversity of a population pool is controlled externally by removing duplicate chromosomes from the current population pool. In this way, chromosomes for the next-generation population pool are selected probabilistically on the basis of their distances from the current chromosome having the highest fitness value. However, the latter chromosome itself is left intact from one generation to the next, as it may indeed be in the vicinity of the global optimum.

The DCGA begins by forming an initial *population pool* $P(0)$ of N candidate chromosomes, obtained by randomly complementing bits in a seed chromosome, where the seed chromosome itself is obtained by using the design variables specific to the optimization problem at hand. Subsequently, the DCGA proceeds to the next-generation population pool $P(t+1)$ from the current-generation population pool

$P(t)$ (with t representing the current generation number, where $t = 0$ initially) as summarized in the following steps [19].

3.1 Design Steps

- To select parents for reproduction, each chromosome in $P(t)$ is chosen only once as a parent. In this way, $N/2$ parent pairs are formed to undergo the genetic operations of crossover and mutation. Two offspring chromosomes are produced per parent pair, resulting in N offspring chromosomes. Let the resulting N offspring chromosomes be represented by $C(t+1)$.
- The chromosomes in $P(t)$ and $C(t+1)$ are combined to form a large population pool $M(t+1)$ of size $2N$. The chromosomes in $M(t+1)$ are evaluated by using a *fitness function*, where the corresponding fitness value signifies how closely the design objectives and/or constraints are satisfied.
- In order to form the next-generation population pool $P(t+1)$, chromosomes in $M(t+1)$ are selected on the basis of a cross-generational probabilistic survival selection (CPSS) [18] scheme as follows:

  1. All chromosomes in $M(t+1)$ which have the same exact bit representation are replaced by one chromosome in order to avoid premature convergence in later generations. This maintains diversity in the population pool.
  2. To form the next-generation population pool $P(t+1)$, the chromosome with the highest fitness value in $P(t)$ is selected at the outset. Subsequently, the CPSS scheme is employed to select as many of the required $N-1$ chromosomes as possible from $M(t+1)$. To this end, if the CPSS scheme leads to fewer chromosomes than required, then the remaining chromosomes are formed by randomly complementing the bits in the chromosome with the highest fitness value in $P(t)$. Conversely, if the CPSS scheme leads to more chromosomes than required, then the first $N-1$ chromosomes are selected. The probability of selection of chromosomes in CPSS is given by

$$p_{\mathrm{s}} = \left[(1-c) * (h/L) + c\right]^{\alpha}, \tag{7}$$

  where L represents the chromosome length, and where h represents the number of bit locations at which a given chromosome differs from the chromosome with the highest fitness value in the population pool (i.e. the *Hamming distance* between the two chromosomes). Moreover, c and α represent control parameters with c representing the shape coefficient and α representing the exponent. The control parameters c and α are used to maintain an external control over the population diversity. In order to avoid premature convergence on the one hand, and to obtain an optimal solution as rapidly as possible on the other, an appropriate level of diversity must be maintained in the population pool. This is achieved by striking a balance between the number of candidate chromosomes which are *quite similar* to or *quite different* from the chromosome with the highest fitness value. As there are no analytical solutions available for c and α, their values must be selected empirically. In particular, if the fitness function has a

few local optima only, then by using a high value of c and/or a small value of α, one can achieve a rapid convergence to an optimal solution. On the other hand, when the fitness function is multimodal, lower values of c and/or higher values of α can be chosen to increase the probability of selecting chromosomes which are different from the chromosome with the highest fitness value. However, we point out that the speed of convergence to an optimal solution is, in general, a function of both c and α values. This implies that one has to empirically find a range of values for c and α in order to achieve rapid convergence [19].

3. A uniform random number is generated between 0 and 1, and if p_s is greater than this random number, then the candidate chromosome is selected for the next-generation population pool (up to a total of N chromosomes).

- The above algorithm is repeated until an appropriate termination condition is reached.

4 DCGA Optimization of FRM FIR Digital Filters

This section is concerned with the application of the DCGA to the development of a novel technique for the design and optimization of FRM FIR digital filters over the CSD multiplier coefficient space.

In his seminal paper [20], Suckley employed the conventional GA for the optimization of finite-precision FIR digital filters, where the seed chromosome was formed by concatenating the binary representation of the constituent multiplier coefficient values. However, in the corresponding case of CSD multiplier coefficients, the initial population pool obtained by complementing the selected bits in the seed chromosome may include chromosomes which violate the CSD number system. The same problem arises under the operations of crossover and mutation in the course of optimization by the underlying GA. In this paper, these problems are resolved *entirely* by employing an indexed look-up table (LUT) of permissible CSD multiplier coefficient values such that the respective set of indices is closed under the GA operations of complementing bits, crossover and mutation. The resulting LUT is similar in concept to that in [25], although derived differently [14].

Based on the above LUT, the seed chromosome is formed by concatenating the binary indices of the CSD multiplier coefficient values (instead of concatenating the ternary representations of the multiplier coefficient values themselves). As a result, the seed chromosome will always result in chromosomes which conform to the original CSD number system due to the closedness of the binary index set.

The proposed DCGA optimization proceeds in a step-by-step manner as follows.

1. *Design of initial infinite-precision FRM FIR digital filter*. The Parks–McClellan approach is employed to design an initial infinite-precision FRM FIR digital filter which satisfies the given design specifications. (We point out that the proposed DCGA can be easily modified to begin with a CSD FRM FIR digital filter at the outset.)

   The design of bandpass and bandstop FRM FIR digital filters is carried out in terms of the corresponding lowpass and highpass FRM digital filters $H_{LP}(z)$ and

$H_{\mathrm{HP}}(z)$, where $H_{\mathrm{LP}}(z)$ and $H_{\mathrm{HP}}(z)$ are themselves designed in terms of the digital sub-filters $H_{\mathrm{al}(h)}(z)$, $H_{\mathrm{mal}(h)}(z)$ and $H_{\mathrm{mbl}(h)}(z)$.

2. *Derivation of CSD LUT*. An LUT of permissible CSD multiplier coefficient values is formed to replace the infinite-precision multiplier coefficient values x_j of the above sub-filters by their corresponding fixed radix point CSD counterparts $\hat{x}_j$ in accordance with

$$\hat{x}_j = \sum_{i=1}^{W} D_{ji} \times 2^{R-i}, \tag{8}$$

where

$$\begin{aligned} &D_{ji} \in \{1,\ -1,\ 0\}, \\ &D_{ji} \times D_{ji+1} = 0, \\ &\sum_{i=1}^{W} |D_{ji}| \leq w, \end{aligned} \tag{9}$$

where W and w have been defined previously, and where the integer R represents a radix point in the range $0 < R < W$. The CSD LUT is formed as a two-column table, with one column including CSD multiplier coefficient values and the other including their respective ordered indices. Let the infinite-precision multiplier coefficient values lie in the range $\{-c_{\mathrm{p}}, +c_{\mathrm{p}}\}$. Moreover, let $W = W_{\mathrm{I}} + W_{\mathrm{F}}$, where W_{I} represents the wordlength of the integer part, and where W_{F} represents the wordlength of the fractional part of the CSD multiplier coefficient values. Then, W_{I} must be chosen such that the integer part of c_{p} can be represented in CSD form without exceeding the wordlength W. W_{F}, on the other hand, must be chosen based on the precision requirements of the FRM FIR digital filter application. Having decided on the values of W and w, the required LUT of CSD numbers is generated exhaustively. The LUT is subsequently trimmed to a size of 2^B, where B is the largest integer such that 2^B is less than or equal to the length of the LUT. In this way, the length of the LUT may have to be enlarged initially, so that, after trimming, the CSD LUT would still be capable of representing the integer part of c_{p} in W_{I} digits.

3. *Generation of seed CSD FRM FIR digital filter*. Having obtained the above indexed CSD LUT, the infinite-precision multiplier coefficient values are quantized to their nearest CSD counterparts in the LUT. Subsequently, the indices of the CSD multiplier coefficient values are converted to B-bit strings and concatenated to form the desired seed CSD FRM FIR digital filter chromosome.
4. *Generation of the population pool*. By manipulating the resulting seed FRM FIR digital filter chromosome, a population pool of N chromosomes is formed by scanning the chromosome B bits (i.e. one index) at a time, and by complementing the bth bit (with $1 \leq b \leq B$, and with $b = 1$ representing the least significant bit) randomly in accordance with the probabilistic relationship $p_{\mathrm{F}} \times 0.5^{B+1-b}$, where p_{F} is a fixed probability factor.
5. *Genetic operations*. The size of the population pool is initially increased from N to $2 \times N$ by using the following genetic operations.

- *Crossover operations*. In the population pool of N chromosomes, $N/2$ pairs of chromosomes are selected as parents so that no chromosome becomes a parent more than once. These chromosome pairs undergo two-point crossover operations, reproducing two offspring chromosomes for each pair. The resulting offspring are then combined with the initial population pool of N chromosomes, enlarging the population pool to $2 \times N$ chromosomes.
- *Mutation operations*. Each member in the population pool of $2 \times N$ chromosomes undergoes mutation operations in accordance with the probabilistic relationship $p_{\mathrm{M}} \times 0.5^{B+1-b}$ to enhance diversity, where p_{M} is the probability of mutation.
- *Fitness evaluation*. The fitness value of each of the $2 \times N$ FRM FIR digital filter chromosomes is evaluated in accordance with

$$\text{fitness}_1 = -20\log\big[\max\{\epsilon_{\mathrm{p}},\ \epsilon_{\mathrm{s}}\}\big] + C, \tag{10}$$

where

$$\epsilon_{\mathrm{p}} = \underbrace{\max}_{\omega\in\Omega_{\mathrm{p}}}\big[W_{\mathrm{p}}\big|H_{\mathrm{LP(HP)}}\big(e^{j\omega}\big) - 1\big|\big] \tag{11}$$

with Ω_{p} representing the passband frequency region(s), and where

$$\epsilon_{\mathrm{s}} = \underbrace{\max}_{\omega\in\Omega_{\mathrm{s}}}\big[W_{\mathrm{s}}\big|H_{\mathrm{LP(HP)}}\big(e^{j\omega}\big)\big|\big] \tag{12}$$

with Ω_{s} representing the stopband frequency region(s). Here, W_{p} and W_{s} are passband and stopband weighting factors, and C is a constant chosen so as to render the fitness_1 value in (10) non-negative. Unfortunately, even the fittest chromosome inferred by fitness_1 in (10) may not necessarily satisfy all the magnitude response specifications. This is mainly due to the *over-optimization* of the magnitude response over certain frequency points in the stopband which occurs at the expense of (drastic) *under-optimization* of the magnitude response over other frequency points.

The over-optimized frequency points in the stopband can be considered as frequency points at which the overall magnitude response attenuation is bounded by a range of attenuations $[A_{\mathrm{l}}, A_{\mathrm{u}}]$ for some suitable A_{l} and A_{u} larger than the specified stopband attenuation. Through empirical investigations it has been found that suitable values for A_{l} and A_{u} are, respectively, 3 dB and 20 dB larger than the specified stopband attenuation.

In order to circumvent the above over-/under-optimization problem, fitness_1 in (10) is modified through the use of a penalty function

$$\text{penalty} = \sum_{i=1}^{P} \frac{|H_{\mathrm{LP(HP)}}(e^{j\omega})|_{\omega\in\widehat{\Omega}_{\mathrm{s}}}}{P} \tag{13}$$

in accordance with

$$\text{fitness}_2 = \text{fitness}_1 - \beta \times \text{penalty}, \tag{14}$$

where $\widehat{\Omega}_s$ represents the set of over-optimized frequency points (with P representing the number of frequency points in $\widehat{\Omega}_s$), and where β is a weighting factor. In this way, the penalty component in (14) penalizes all the stopband frequency points in $\widehat{\Omega}_s$ by rendering the respective chromosome less fit.

At the completion of fitness evaluation, the chromosomes are ranked and duplicate chromosomes are eliminated to avoid affecting diversity adversely. In the event that the resulting population pool does not contain a chromosome that satisfies the given design magnitude response specifications, the DCGA optimization proceeds to generate the next-generation population pool. Otherwise, it terminates with the highest ranked chromosome declared as optimum.

6. The next-generation population pool is formed by using the CPSS in (7), where the parameter L is given by

$$L = \left(N_{\mathrm{al}(h)} + N_{\mathrm{mal}(h)} + N_{\mathrm{mbl}(h)}\right) \times B, \tag{15}$$

and where $N_{\mathrm{al}(h)}$, $N_{\mathrm{mal}(h)}$ and $N_{\mathrm{mbl}(h)}$ are the number of multiplier coefficients in the sub-filters $H_{\mathrm{al}(h)}(z)$, $H_{\mathrm{mal}(h)}(z)$ and $H_{\mathrm{mbl}(h)}(z)$, respectively. The selected chromosome is chosen as a candidate for the next-generation population pool if p_S is greater than a locally generated uniform random number. This process is repeated until N chromosomes are identified for the next-generation population pool.

5 Application Examples

In this section, the proposed DCGA is applied to the design and optimization of a pair of bandpass FRM FIR digital filters, one having equal and the other having arbitrary lower and upper transition bandwidths Δ_l and Δ_h. We point out that in the case of $\Delta_l = \Delta_u$, it may be more efficient to realize the bandpass FRM FIR digital filter *directly* as in [14]. Empirical investigations are also undertaken to identify appropriate ranges of values for the DCGA control parameters c and α.

5.1 Bandpass FRM FIR Digital Filter for the Case of $\Delta_l = \Delta_u$

Let us consider the design and optimization of a bandpass FRM FIR digital filter satisfying the following magnitude response specifications for implementation over the CSD multiplier coefficient space:

Passband region	$0.21\pi \le \omega \le 0.6\pi$	
Lower stopband region	$0 \le \omega \le 0.2\pi$	
Upper stopband region	$0.61 \le \omega \le \pi$	(16)
Maximum passband ripple	± 0.1 dB	
Minimum stopband attenuation	40 dB	

The above specifications can be easily recast into specifications for the constituent lowpass and highpass FRM FIR digital filters $H_{\mathrm{LP}}(z)$ and $H_{\mathrm{HP}}(z)$ as shown in (17) and (18).

Table 1 Digital sub-filter orders for various values of M for the case $\Delta_l = \Delta_u$

M	H_{al}	H_{mal}	H_{mbl}	H_{ah}	H_{mah}	H_{mbh}	Total order
2	254	24	2	234	10	6	530
3	168	8	42	156	10	18	402
4	126	16	24	118	10	52	346
5	102	506	12	94	10	468	1192
6	**84**	**24**	**42**	**78**	**18**	**62**	**308**
7	72	22	86	68	30	38	316

Table 2 Bandedge frequencies for digital sub-filters $H_{al(h)}(z)$, $H_{mal(h)}(z)$ and $H_{mbl(h)}(z)$ for the case $\Delta_l = \Delta_u$

Sub-filter	Passband edge frequencies	Stopband edge frequencies
$H_{al}(e^{j\omega})$	0.34π	0.4π
$H_{mal}(e^{j\omega})$	0.4π	0.61π
$H_{mbl}(e^{j\omega})$	0.6π	0.72π
$H_{ah}(e^{j\omega})$	0.8π	0.74π
$H_{mah}(e^{j\omega})$	0.46π	0.2π
$H_{mbh}(e^{j\omega})$	0.21π	0.13π

Design Specifications for Lowpass FRM FIR Digital Filter $H_{LP}(z)$

$$\begin{array}{ll} \text{Passband region} & 0 \le \omega \le 0.6\pi \\ \text{Stopband region} & 0.61\pi \le \omega \le \pi \\ \text{Maximum passband ripple} & \pm 0.1 \text{ dB} \\ \text{Minimum stopband attenuation} & 40 \text{ dB} \end{array} \tag{17}$$

Design Specifications for Highpass FRM FIR Digital Filter $H_{HP}(z)$

$$\begin{array}{ll} \text{Passband region} & 0.21\pi \le \omega \le \pi \\ \text{Stopband region} & 0 \le \omega \le 0.2\pi \\ \text{Maximum passband ripple} & \pm 0.1 \text{ dB} \\ \text{Minimum stopband attenuation} & 40 \text{ dB} \end{array} \tag{18}$$

In this case, $M_{LP} = M_{HP} \equiv M$ because of equal lower and upper transition bandwidths Δ_l and Δ_u. By using (6) with $\alpha = 2.4$, the first approximation to the optimum value of the interpolation factor M is obtained as 4. Table 1 shows the overall bandpass FRM FIR digital filter order as a function of interpolation factor M in the vicinity of the first approximation for M. Through inspection of Table 1, the optimum value of M is found to be 6, yielding digital sub-filters $H_{al}(z)$, $H_{mal}(z)$, $H_{mbl}(z)$, $H_{ah}(z)$, $H_{mah}(z)$ and $H_{mbh}(z)$ of orders 84, 24, 42, 78, 18 and 62, respectively.

Having determined the required digital sub-filter orders, their bandedge frequencies can be determined as given in Table 2 [8, 21]. Moreover, the corresponding

Table 3 Passband ripples and stopband attenuations associated with digital sub-filters $H_{\mathrm{al}(h)}(z)$, $H_{\mathrm{mal}(h)}(z)$ and $H_{\mathrm{mbl}(h)}(z)$ for bandpass FRM FIR digital filter for $\Delta_{\mathrm{l}} = \Delta_{\mathrm{u}}$

Sub-filter	Passband ripple	Stopband attenuation
$H_{\mathrm{al}}(e^{j\omega})$	0.085 dB	−46 dB
$H_{\mathrm{mal}}(e^{j\omega})$	0.085 dB	−46 dB
$H_{\mathrm{mbl}}(e^{j\omega})$	0.085 dB	−46 dB
$H_{\mathrm{ah}}(e^{j\omega})$	0.085 dB	−46 dB
$H_{\mathrm{mah}}(e^{j\omega})$	0.085 dB	−46 dB
$H_{\mathrm{mbh}}(e^{j\omega})$	0.085 dB	−46 dB

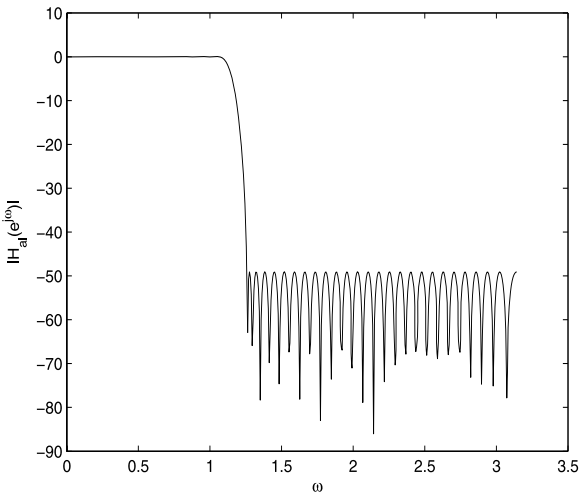

Fig. 4 Magnitude response of the digital sub-filter $H_{\mathrm{al}}(z)$ for the bandpass case with $\Delta_{\mathrm{l}} = \Delta_{\mathrm{u}}$

maximum passband ripples and minimum stopband attenuations are set as given in Table 3. These set values are obtained as 85% of their budgeted values as given in (16) (so as to compensate for any second-order effects).

By using the Parks–McClellan approach in connection with the design specifications in Tables 2 and 3, the initial infinite-precision digital sub-filters $H_{\mathrm{al}}(z)$, $H_{\mathrm{mal}}(z)$, $H_{\mathrm{mbl}}(z)$, $H_{\mathrm{ah}}(z)$, $H_{\mathrm{mah}}(z)$ and $H_{\mathrm{mbh}}(z)$ are designed to have the magnitude frequency responses as shown in Figs. 4, 5, 6, 7, 8, 9, 10, 11, 12, 13, and the corresponding overall infinite-precision bandpass FRM FIR digital filter is obtained to have a magnitude frequency response as shown in Fig. 14.

The DCGA optimization parameters for obtaining the desired bandpass CSD FRM FIR digital filter are as summarized in Table 4. By quantizing the multiplier coefficients of the infinite-precision FRM FIR digital filter to their nearest counterparts in the CSD LUT, one can obtain a seed bandpass CSD FRM FIR digital filter having a magnitude frequency response as shown in Fig. 15. This magnitude frequency response violates the design specifications in (16) by almost 0.5 dB in the passband, and by almost 20 dB in the stopband region (cf. Table 5).

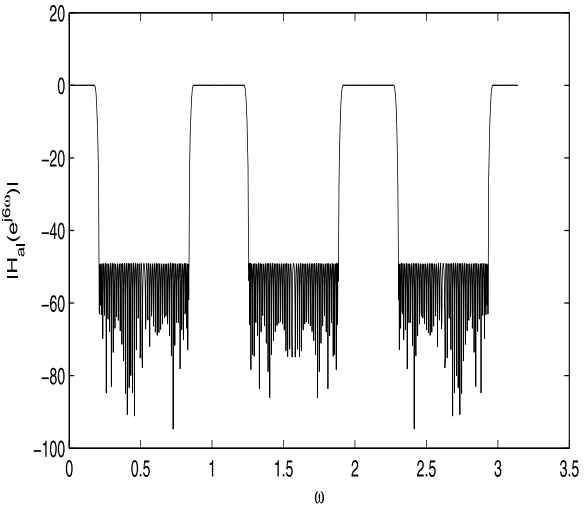

Fig. 5 Magnitude response of the M-interpolated version of $H_{\mathrm{al}}(z)$ for the bandpass case with $\Delta_{\mathrm{l}} = \Delta_{\mathrm{u}}$

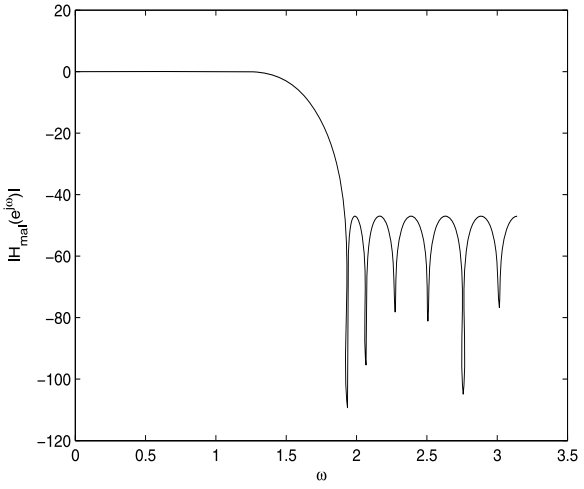

Fig. 6 Magnitude response of the masking digital sub-filter $H_{\mathrm{mal}}(z)$ for the bandpass case with $\Delta_{\mathrm{l}} = \Delta_{\mathrm{u}}$

Before proceeding with the DCGA optimization, one must determine appropriate values for the control parameters c and α. Fig. 16 shows the convergence speed of the DCGA optimization for the value of the shaping parameter c ranging from 0.1 to 0.5, and for the value of the exponent parameter α ranging from 0.1 to 0.3. In this way, the fastest convergence speed is observed to occur at $c = 0.5$ and $\alpha = 0.2$. For completeness, Fig. 17 shows the convergence speed for various values of the parameter c averaged over the value of the parameter α. Consequently, on average, one can obtain high convergence speeds for c ranging from 0.3 to 0.5.

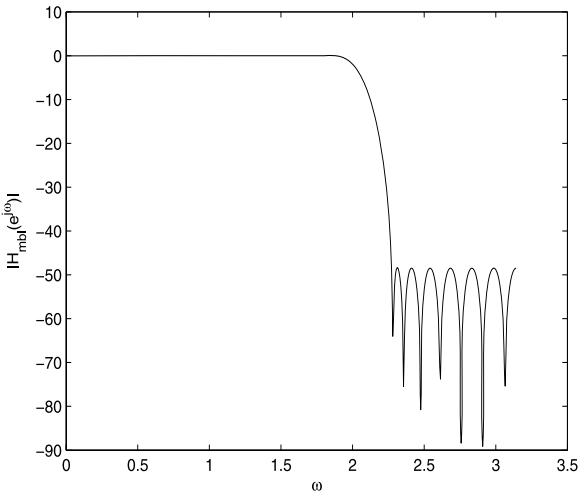

Fig. 7 Magnitude response of the masking digital sub-filter $H_{\mathrm{mbl}}(z)$ for the bandpass case with $\Delta_{\mathrm{l}} = \Delta_{\mathrm{u}}$

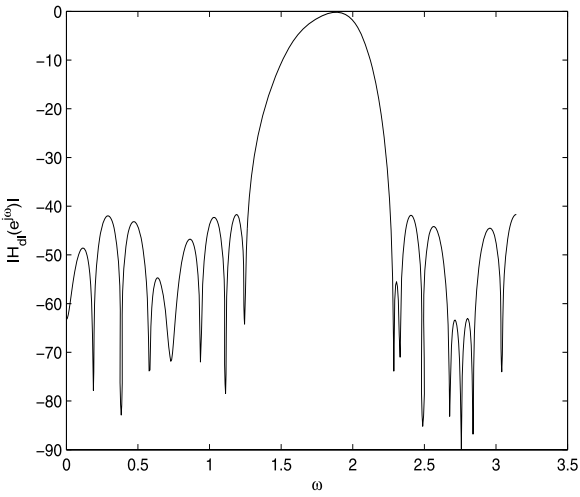

Fig. 8 Magnitude response of the masking digital sub-filter $H_{\mathrm{dl}}(z)$ for the bandpass case with $\Delta_{\mathrm{l}} = \Delta_{\mathrm{u}}$

For $c = 0.5$ and $\alpha = 0.2$, the DCGA optimization converges to the corresponding optimal bandpass CSD FRM FIR digital filter after 144 generations, resulting in a magnitude frequency response as shown in Fig. 18 and enlarged over the passband region in Fig. 19.

By comparing the DCGA to the corresponding conventional GA for the optimization of bandpass FRM FIR digital filters [14], it has been observed that the DCGA leads to convergence speeds which are around an order of magnitude higher than those of the conventional GA. For example, by using the conventional GA in [14],

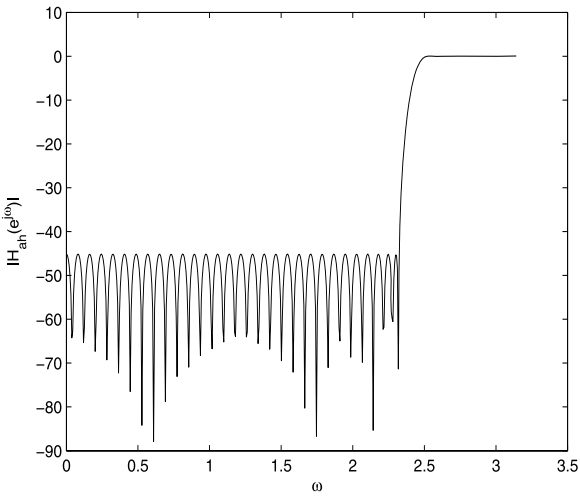

Fig. 9 Magnitude response of the digital sub-filter $H_{\mathrm{ah}}(z)$ for the bandpass case with $\Delta_{\mathrm{l}} = \Delta_{\mathrm{u}}$

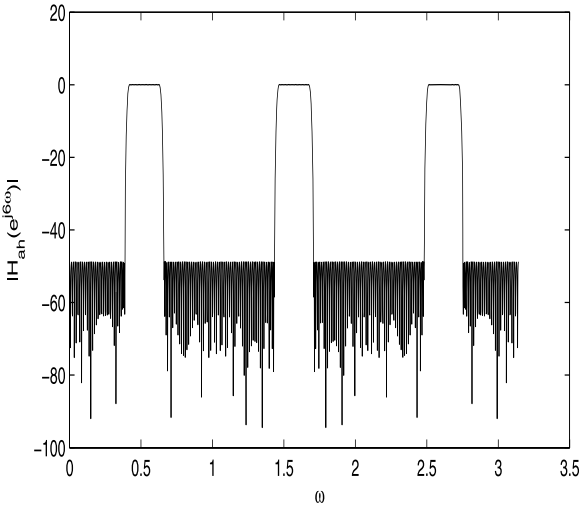

Fig. 10 Magnitude response of the M-interpolated version of $H_{\mathrm{ah}}(z)$ for the bandpass case with $\Delta_{\mathrm{l}} = \Delta_{\mathrm{u}}$

it took 1000 generations to arrive at a bandpass FRM FIR digital filter, whereas the proposed DCGA took only 144 generations (for similar design specifications).

5.2 Bandpass FRM FIR Digital Filter for the Case of $\Delta_{\mathrm{l}} \neq \Delta_{\mathrm{u}}$

Let us consider the design and optimization of a bandpass FRM FIR digital filter with unequal transition bandwidths Δ_{l} and Δ_{u}, satisfying the following magnitude

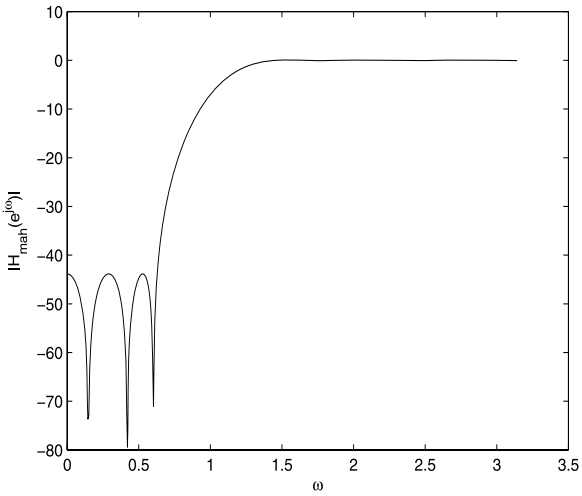

Fig. 11 Magnitude response of the masking digital sub-filter $H_{\mathrm{mah}}(z)$ for the bandpass case with $\Delta_{\mathrm{l}} = \Delta_{\mathrm{u}}$

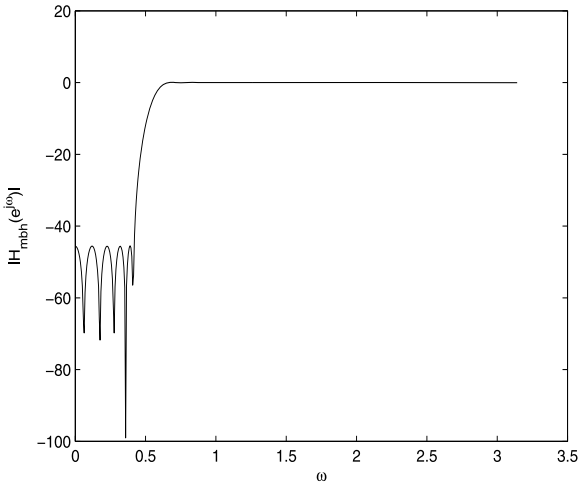

Fig. 12 Magnitude response of the masking digital sub-filter $H_{\mathrm{mbh}}(z)$ for the bandpass case with $\Delta_{\mathrm{l}} = \Delta_{\mathrm{u}}$

response specifications over the CSD multiplier coefficient space:

Passband region	$0.33\pi \le \omega \le 0.6\pi$	
Lower stopband region	$0 \le \omega \le 0.3\pi$	
Upper stopband region	$0.61 \le \omega \le \pi$	(19)
Maximum passband ripple	± 0.1 dB	
Minimum stopband attenuation	40 dB	

The above specifications can be recast into corresponding specifications for the constituent lowpass and highpass FRM FIR digital filters $H_{\mathrm{LP}}(z)$ and $H_{\mathrm{HP}}(z)$ in much the same way as before. In this case, because of unequal lower and upper transition

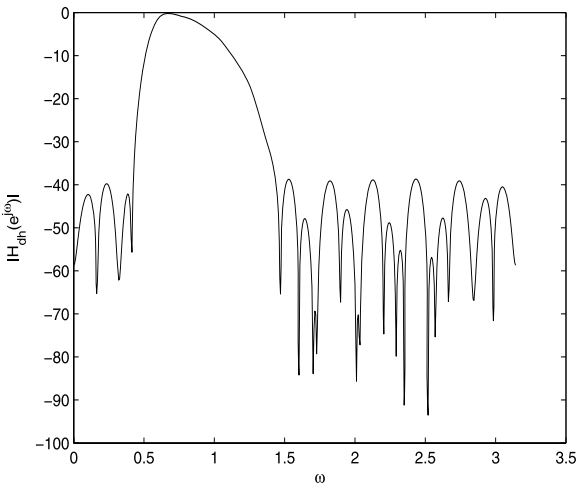

Fig. 13 Magnitude response of the masking digital sub-filter $H_{\mathrm{dh}}(z)$ for the bandpass case with $\Delta_{\mathrm{l}} = \Delta_{\mathrm{u}}$

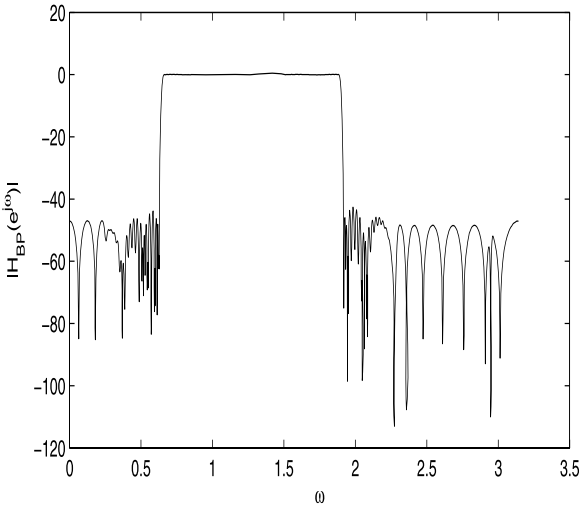

Fig. 14 Magnitude response of the infinite-precision bandpass FRM FIR digital filter with $\Delta_{\mathrm{l}} = \Delta_{\mathrm{u}}$

Table 4 Design parameters for DCGA optimization of CSD bandpass FRM FIR digital filter for the case $\Delta_{\mathrm{l}} = \Delta_{\mathrm{u}}$

Design step	Design parameters
1	$M = 6,\ N_{\mathrm{al}} = 84,\ N_{\mathrm{mal}} = 24,\ N_{\mathrm{mbl}} = 42,\ N_{\mathrm{ah}} = 78,\ N_{\mathrm{mah}} = 18,\ N_{\mathrm{mbh}} = 62$
2	$w = 3$ digits, $W_{\mathrm{I}} = 3$ digits, $W_{\mathrm{F}} = 14$ digits, $B = 12$ bits
3	$p_{\mathrm{F}} = 0.8,\ N = 500$
4	$C = 30,\ W_{\mathrm{p}} = 1.15,\ W_{\mathrm{s}} = 0.85,\ \beta = 100,\ T_{\mathrm{u}} = 0.0005,\ T_{\mathrm{l}} = 0.008$
5	$L = 3696$

Table 5 Bandpass CSD FRM FIR digital filter magnitude response characteristics for the case $\Delta_l = \Delta_u$ before and after DCGA optimization

Multiplier coefficient representation	Passband ripple	Lower stopband attenuation	Upper stopband attenuation
Infinite-Precision	0.075 dB	−41 dB	−42.8 dB
CSD before DCGA optimization	1.12 dB	−22.3 dB	−24.15 dB
CSD after DCGA optimization	0.1 dB	−42.2 dB	−41.9 dB

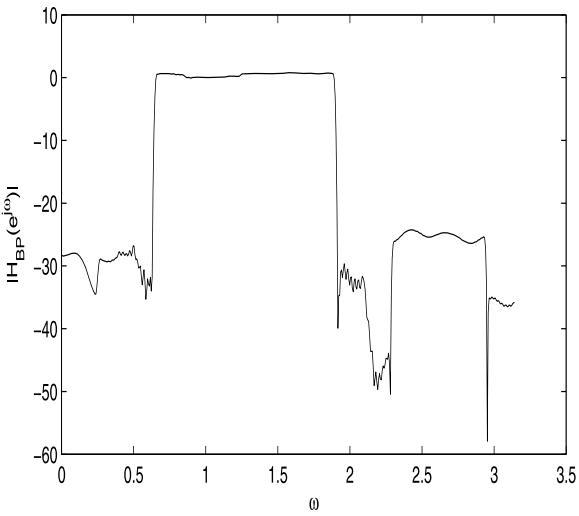

Fig. 15 Magnitude response of the bandpass CSD FRM FIR digital filter with $\Delta_l = \Delta_u$ before DCGA optimization

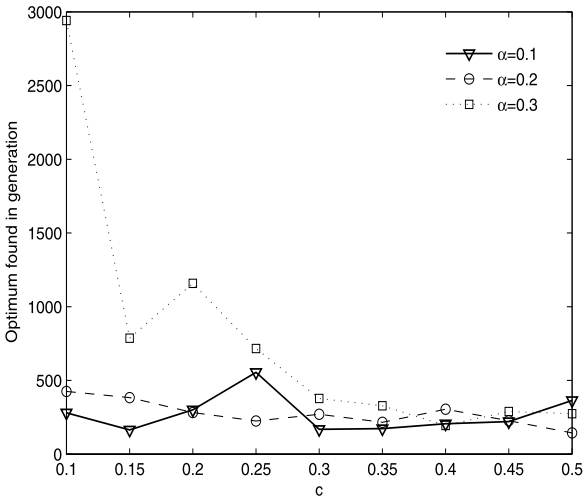

Fig. 16 DCGA convergence speed for bandpass FRM FIR digital filter with $\Delta_l = \Delta_u$ for varying c and α

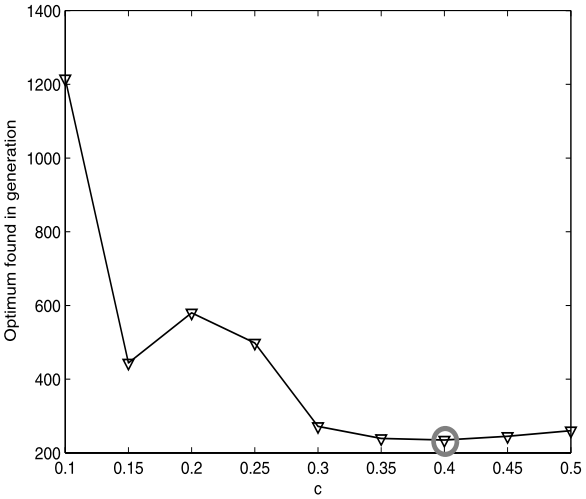

Fig. 17 Average DCGA convergence speed for bandpass FRM FIR digital filter with $\Delta_l = \Delta_u$ for varying c

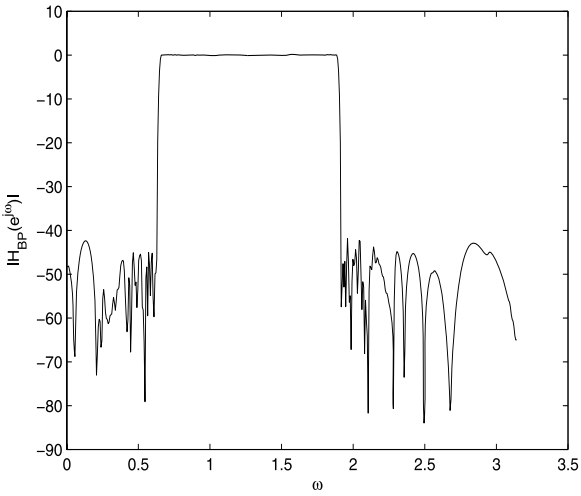

Fig. 18 Magnitude response of the CSD bandpass FRM FIR digital filter with $\Delta_l = \Delta_u$ after DCGA optimization

bandwidths Δ_l and Δ_u, by using (6) with $\alpha = 2.4$, the first approximations to the optimum values of the interpolation factors M_{LP} and M_{HP} are obtained as 3 and 2, respectively. Tables 6, 7 show the order of the constituent lowpass (highpass) FRM FIR digital filter $H_{LP(HP)}(z)$ as a function of the interpolation factor $M_{LP(HP)}$ in the vicinity of its first approximation for $M_{LP(HP)}$. Through inspection of Tables 6 and 7, the optimum values of M_{LP} and M_{HP} are found to be 6 and 5 respectively, yielding FRM FIR digital sub-filters $H_{al}(z)$, $H_{mal}(z)$, $H_{mbl}(z)$, $H_{ah}(z)$, $H_{mah}(z)$ and $H_{mbh}(z)$ of orders 84, 24, 42, 34, 30 and 22, respectively. Table 8 shows the bandedge frequency specifications for these digital sub-filters, obtained by using the design equations in [8] and [21]. Moreover, the corresponding passband ripples and stopband

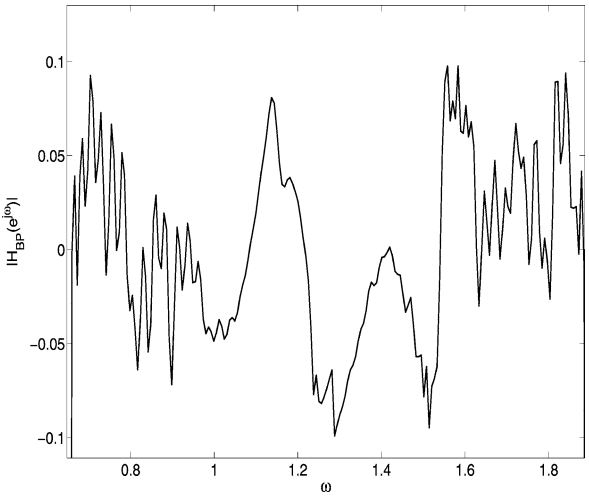

Fig. 19 Passband of CSD bandpass FRM FIR digital filter with $\Delta_l = \Delta_u$ after DCGA optimization

Table 6 Digital sub-filter orders for the constituent lowpass FRM FIR digital filter $H_{LP}(z)$ for various values of M_{LP} for the case $\Delta_l \neq \Delta_u$

M	H_{al}	H_{mal}	H_{mbl}	Total multiplication
2	254	24	2	280
3	168	8	42	218
4	126	16	24	166
5	102	506	12	620
6	**84**	**24**	**42**	**150**
7	72	22	76	170

Table 7 Digital sub-filter orders for the constituent highpass FRM FIR digital filter $H_{HP}(z)$ for various values of M_{HP} for the case $\Delta_l \neq \Delta_u$

M	H_{ah}	H_{mah}	H_{mbh}	Total multiplication
2	84	6	12	102
3	56	6	138	200
4	42	12	40	94
5	**34**	**30**	**22**	**86**
6	28	138	16	182
7	24	86	22	132
8	20	40	42	102

attenuations are set in Table 9. By using the design specifications in Tables 8 and 9, the Parks–McClellan approach is employed to obtain the overall infinite-precision bandpass FRM FIR digital filter $H_{BP}(z)$ having a magnitude frequency response as shown in Fig. 20.

Table 8 Bandedge frequencies for digital sub-filters $H_{\mathrm{al}(h)}(z)$, $H_{\mathrm{mal}(h)}(z)$ and $H_{\mathrm{mbl}(h)}(z)$ for the case $\Delta_{\mathrm{l}} \neq \Delta_{\mathrm{u}}$

Sub-filter	Passband edge frequencies	Stopband edge frequencies
$H_{\mathrm{al}}(e^{j\omega})$	0.34π	0.4π
$H_{\mathrm{mal}}(e^{j\omega})$	0.4π	0.61π
$H_{\mathrm{mbl}}(e^{j\omega})$	0.6π	0.72π
$H_{\mathrm{ah}}(e^{j\omega})$	0.5π	0.35π
$H_{\mathrm{mah}}(e^{j\omega})$	0.47π	0.3π
$H_{\mathrm{mbh}}(e^{j\omega})$	0.33π	0.1π

Table 9 Passband ripples and stopband attenuations associated with digital sub-filters $H_{\mathrm{al}(h)}(z)$, $H_{\mathrm{mal}(h)}(z)$ and $H_{\mathrm{mbl}(h)}(z)$ for bandpass FRM FIR digital filter for $\Delta_{\mathrm{l}} \neq \Delta_{\mathrm{u}}$

Sub-filter	Passband ripple	Stopband attenuation
$H_{\mathrm{al}}(e^{j\omega})$	0.085 dB	−46 dB
$H_{\mathrm{mal}}(e^{j\omega})$	0.085 dB	−46 dB
$H_{\mathrm{mbl}}(e^{j\omega})$	0.085 dB	−46 dB
$H_{\mathrm{ah}}(e^{j\omega})$	0.085 dB	−46 dB
$H_{\mathrm{mah}}(e^{j\omega})$	0.085 dB	−46 dB
$H_{\mathrm{mbh}}(e^{j\omega})$	0.085 dB	−46 dB

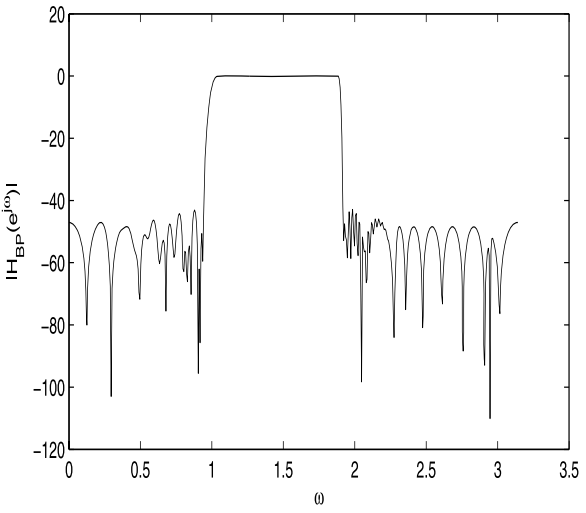

Fig. 20 Magnitude response of the infinite-precision bandpass FRM FIR digital filter with $\Delta_{\mathrm{l}} \neq \Delta_{\mathrm{u}}$

Table 10 summarizes the design parameters for the DCGA optimization of the seed infinite-precision bandpass CSD FRM FIR digital filter with unequal lower and upper transition bandwidths Δ_{l} and Δ_{u}. Fig. 21 shows the magnitude frequency response of the seed bandpass CSD FRM FIR digital filter after the infinite-precision multiplier coefficients have been quantized to their nearest CSD counterparts in the LUT. This

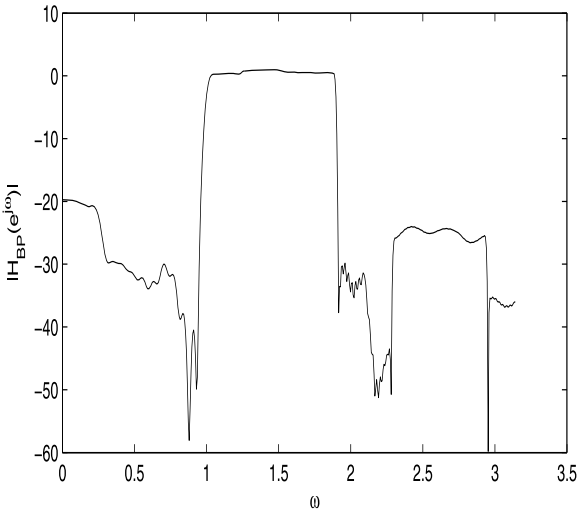

Fig. 21 Magnitude response of the bandpass FRM FIR digital filter with $\Delta_l \neq \Delta_u$ before DCGA optimization

Table 10 Design parameters for DCGA optimization of CSD bandpass FRM FIR digital filter for the case $\Delta_l \neq \Delta_u$

Design step	Design parameters
1	$M_{LP} = 6,\ N_{al} = 84,\ N_{mal} = 24,\ N_{mbl} = 42,$ $M_{HP} = 5,\ N_{ah} = 34,\ N_{mah} = 30,\ N_{mbh} = 22$
2	$w = 3$ digits, $W_I = 3$ digits, $W_F = 14$ digits, $B = 12$ bits
3	$p_F = 0.8,\ N = 500$
4	$C = 30,\ W_p = 1.15,\ W_s = 0.85,\ \beta = 100,\ T_u = 0.0005,\ T_l = 0.008$
5	$L = 2832$

Table 11 Bandpass CSD FRM FIR digital filter magnitude responses for the case $\Delta_l \neq \Delta_u$ before and after DCGA optimization

Multiplier coefficient representation	Passband ripple	Lower stopband attenuation	Upper stopband attenuation
Infinite-precision	0.093 dB	−43 dB	−42.8 dB
CSD before DCGA optimization	0.98 dB	−20 dB	−24 dB
CSD after DCGA Optimization	0.1 dB	−43 dB	−42.3 dB

magnitude frequency response violates the design specifications in (19) by almost 0.9 dB in the passband, and by around 20 dB in the stopband region (cf. Table 11).

The convergence speed of the DCGA optimization for the values of shaping parameter c ranging from 0.1 to 0.5 and for the values of exponent parameter α ranging from 0.1 to 0.3 is shown in Fig. 22. Consequently, the fastest convergence speed is

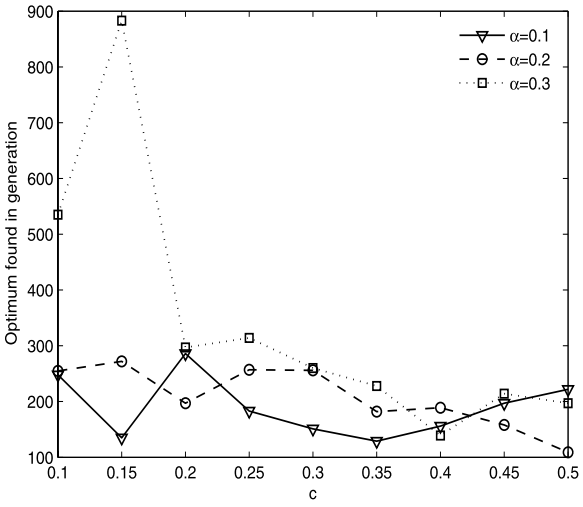

Fig. 22 DCGA convergence speed for bandpass FRM FIR digital filter with $\Delta_l \neq \Delta_u$ for varying c and α

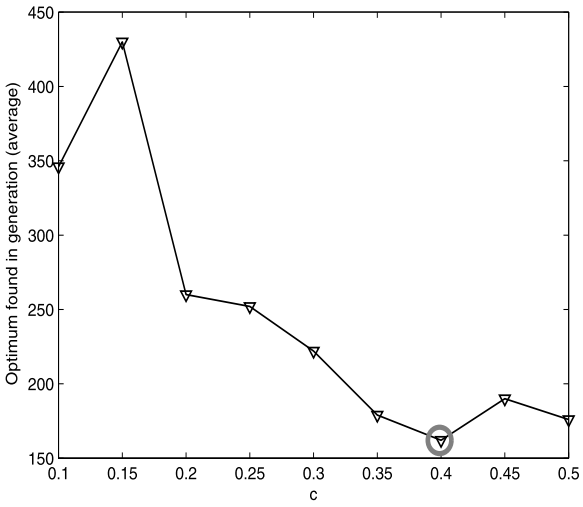

Fig. 23 Average DCGA convergence speed for bandpass FRM FIR digital filter with $\Delta_l \neq \Delta_u$ for varying c

observed to occur at $c = 0.5$ and $\alpha = 0.2$. Once again, for completeness, the convergence speed for various values of the parameter c averaged over the value of the parameter α is shown in Fig. 23. Consequently, on average, one can obtain high convergence speeds for c ranging from 0.3 to 0.5. In this way, for $c = 0.5$ and $\alpha = 0.2$, the optimal bandpass CSD FRM FIR digital filter is obtained after 109 generations having a magnitude frequency response as shown in Fig. 24 and enlarged over the passband region in Fig. 25.

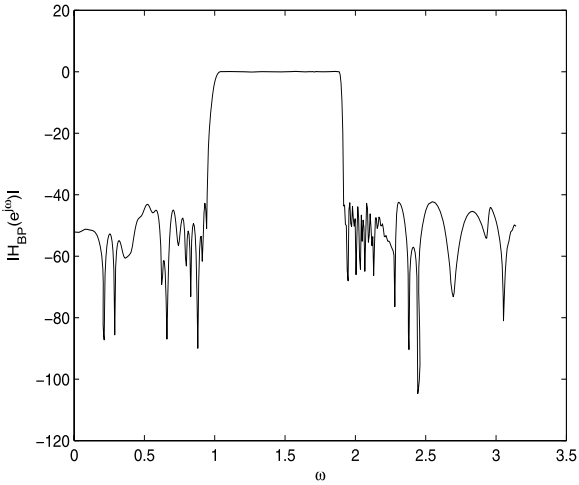

Fig. 24 Magnitude response of the CSD bandpass FRM FIR digital filter with $\Delta_l \neq \Delta_u$ after DCGA optimization

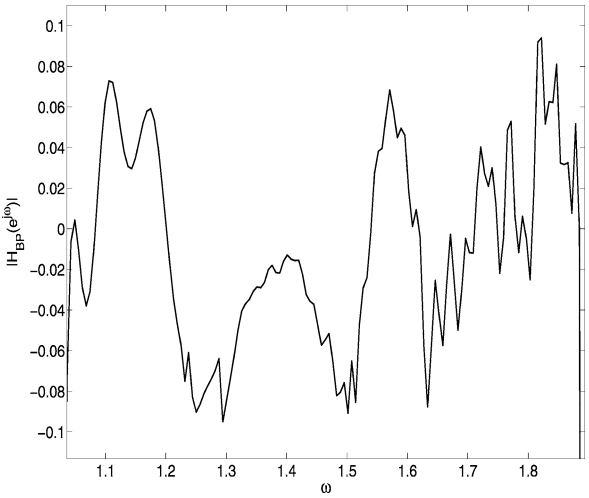

Fig. 25 Passband of CSD bandpass FRM FIR digital filter with $\Delta_l \neq \Delta_u$ after DCGA optimization

6 Concluding Remarks

A novel DCGA has been presented for the discrete optimization of bandpass FRM FIR digital filters over the CSD multiplier coefficient space. The resulting bandpass FIR digital filters are permitted to have equal or unequal lower and upper transition bandwidths. A cross-generational probabilistic survival selection scheme has been employed to form the next-generation population pool in the course of DCGA optimization. Two application examples have been given, one involving DCGA optimization of a bandpass FRM digital filter having equal lower and upper transition bandwidths, and the other involving that of a bandpass FRM FIR digital filter hav-

ing unequal lower and upper transition bandwidths. Empirical investigations have been undertaken to determine the DCGA control parameters for achieving rapid convergence speeds. These empirical values have led to convergence speeds which are around an order of magnitude higher than those of the conventional GAs. The proposed DCGA can be easily modified to begin with a finite-precision (CSD) FRM FIR digital filter instead of an infinite-precision FRM digital filter (usually obtained by employing the Parks–McClellan approach).

Acknowledgement This work was supported, in part, by a Natural Science and Engineering Research Council of Canada under Discovery Grant #A6715.

References

1. L. Cen, Y. Lian, Hybrid genetic algorithm for the design of modified frequency-resposne masking filters in a discrete space. Circuits Syst. Signal Process. **25**(2), 153–174 (2006)
2. V.S. Dimitrov, G.A. Jullien, Loading the bases: A new number representation with applications, Technical report, IEEE Circuits and Systems Magazine, 2003
3. A.T.G. Fuller, B. Nowrouzian, F. Ashrafzadeh, Optimization of fir digital filters over the canonical signed-digit coefficient space using genetic algorithms, in *Midwest Symposium on Circuits and Systems* (1998), pp. 456–469
4. D.E. Goldberg, *Genetic Algorithms in Search, Optimization, and Maching Learning* (Addison-Wesley, Reading, 1989)
5. O. Hermann, L.R. Rabiner, D.S.K. Chan, Practical design rules for optimum finite impulse response lowpass digital filters. Bell Syst. Tech. J. **52**, 769–799 (1981)
6. W.R. Lee, V. Rehbock, K.L. Teo, Frequency-response masking based fir filter design with power-of-two coefficients and suboptimum pwr. J. Circuits Syst. Comput. **12**(5), 591–600 (2003)
7. Y.C. Lim, A digital filter bank for digital audio systems. IEEE Trans. Circuits Syst. **33**(8), 848–849 (1986)
8. Y.C. Lim, Frequency-response masking approach for the synthesis of sharp linear phase digital filters. IEEE Trans. Circuits Syst. **CAS-33**, 357–364 (1986)
9. Y.C. Lim, Y. Lian, The optimum design of one- and two-dimensional fir filters using the frequency response masking technique. IEEE Trans. Circuits Syst. II **CAS-40**, 88–95 (1993)
10. Y.C. Lim, S.R. Parker, A.G. Constantinides, Finite word length fir filter design using integer programming over a discrete coefficient space. IEEE Trans. Acoust. Speech Signal Process **ASSP-30**, 661–664 (1982)
11. Y.C. Lim, R. Yang, D. Li, J. Song, Signed power-of-two term allocation scheme for the design of digital filters. IEEE Trans. Circuits Syst. Analog Digit. Signal Process. **II**, 577–584 (1999)
12. W. Lu, T. Hinamoto, Optimal design of frequency-response-masking filters using semidefinite programming. IEEE Trans. Circuits Syst. **5**, 557–568 (2003)
13. W. Lu, T. Hinamoto, Improved design of frequency-response-masking filters using enhanced sequential quadratic programming. IEEE Int. Symp. Circuits Syst. **5**, 528–531 (2004)
14. P. Mercier, S. Mohan-Kilambi, B. Nowrouzian, Optimization of frm fir digital filters over csd and dbns multiplier coefficient spaces employing a novel genetic algorithm. J. Comput. **2**(7), 20–31 (2007)
15. S.K. Mitra, *Digital Signal Processing—A Computer-Based Approach* (McGraw Hill, New York, 2006)
16. Y. Neuvo, C.Y. Dong, S.K. Mitra, Interpolated finite impulse response filters. IEEE. Trans. Acoust. Speech Signal Process. **ASSP-32**, 563–570 (1984)
17. T. Saramaki, J. Yli-Kaakinen, H. Johansson, Optimization of frequency-response making based fir filters. J. Circuits Syst. Comput. **12**(5), 563–591 (2003)
18. H. Shimodaira, Dcga: a diversity control oriented genetic algorithm, in *Proceedings on Ninth IEEE International Conference on Tools with Artificial Intelligence* (1997), pp. 367–374
19. H. Shimodaira, A diversity-control-oriented genetic algorithm (dcga): Performance in function optimization, in *Proceedings of the 2001 Congress on Evolutionary Computation*, vol. 1 (2001), pp. 44–51

20. D. Suckley, Genetic algorithm in the design of fir filters. IEEE Proc. G **138**, 234–238 (1991)
21. R. Yang, Y.C. Lim, S.R. Parker, Design of sharp linear-phase fir bandstop filters using the frequency response-masking technique. Circuits Syst. Signal Process. **17**, 1–27 (1998)
22. J.H. Yu, Y. Lian, Design equations for jointly optimized frequency-resposne masking filters. Circuits Syst. Signal Process. **26**(1), 27–42 (2007)
23. Y.J. Yu, Y.C. Lim, Frm based fir filter design—the wls approach. IEEE Int. Symp. Circuits Syst. **III**, 221–224 (2002)
24. Y.J. Yu, Y.C. Lim, Genetic algorithm approach for the optimization of multiplierless sub-filters generated by the frequency response masking technique, in *IEEE International Conference on Electronics, Circuits and Systems*, vol. 3 (2002), pp. 1163–1166
25. Y.J. Yu, Y.C. Lim, A novel genetic algorithm for the design of a signed power-of-two coefficient quadrature mirror filter lattice filter bank. Circuits Syst. Signal Process. **21**, 263–276 (2002)